Analytical model of transcritical diffusion flame in a turbulent coaxial jet

A. Genot[a], M. Bouton[b,c], L. Sanchez[b,d], H. Bezard[a]

[a]DMPE, ONERA, Université de Toulouse, 31000, Toulouse, France

[b]DMPE, ONERA, Université Paris-Saclay, 91120, Palaiseau, France

[c]CNES – Transport Spatial – Etablissement de Daumesnil, F-75612, Paris Cedex, France

[d]Institut de Mécanique des Fluides de Toulouse, IMFT, CNRS, Université de Toulouse, Toulouse, France

1 Introduction

In the context of space competition, innovations with a decreasing cost of technology development are one of the prospects. In the process of system design, experimental tests and numerical simulations are usually carried out. The quantity of experimental tests has already been reduced in these processes, with the help of increasing capacities of numerical simulations [1]. However, numerical simulation campaigns reach costs comparable to experimental tests with always questionable results and a limited map of operating regimes. Analytical (or semi-analytical) models are usually crude but have very low computation cost in comparison with high-order numerical simulations. To design a Liquid Rocket Engine (LRE), two criteria must be met: (1) satisfactory engine thrust (good performance) and (2) duration of the mission in complete safety (no engine failure). Both are directly related to combustion dynamics. These engines are equipped with a significant number of injectors, with a flame attached downstream of each of the injectors (as illustrated in Fig. 1). For each injector, the first criterion requires a model of the time-average heat release rate induced by the flame. The second criterion needs to model the unsteady behavior of the flame, which is also related to its time-average value [2–4]. In this study, we propose an original model for the time-average heat release rate of a liquid rocket injector in transcritical regime. Such model can be implemented to design a complete liquid rocket engine.

The second section deals with the features of the flow and the assumptions useful for the model, which is developed in the third section. Finally, a validation of the model with numerical simulation data is presented in the last section before the conclusion.

2 Flow characteristics and assumptions

To validate our analytical model, two large eddy simulations (LES) are considered [2, 4]. Both are simulating the same operating point. The first, realized by Nez *et al.* [2] is in three dimensions, while the second, by Bouton *et al.* [4] is in two dimensions (cylindrical coordinate system).

Some instantaneous fields of 3D LES [2] are illustrated in Figs. 1a and 1b. Liquid oxygen (LOx), represented in black, is injected in the center of the jet and remains liquid up to positions very far from the injector ($x/r_{LO_x} < 40$). The dense phase should certainly perturb the development of jet turbulence [12]. Indeed, the width of the reactive zone, represented by the red-orange-yellow gradient in Fig. 1b, seems quite constant, at least close to the injection. Fig. 1c represents the simplified geometry, without a lip, for the analytical model derived in the following.

Some useful assumptions are listed below, based on previous observations and state-of-the-art analyses.

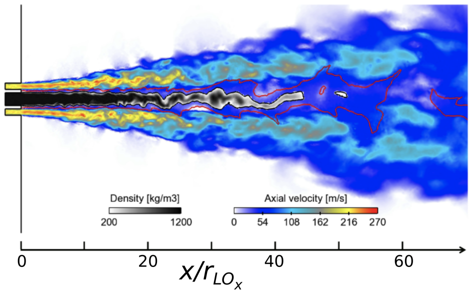

(a) Typical flow dynamics [2]

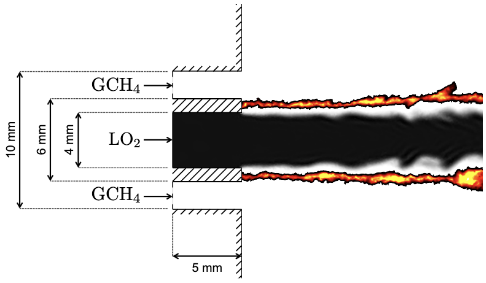

(b) Transverse slice close to the injector of an instantaneous LES field: dense phase in black and flame in red-orange-yellow gradient [2]

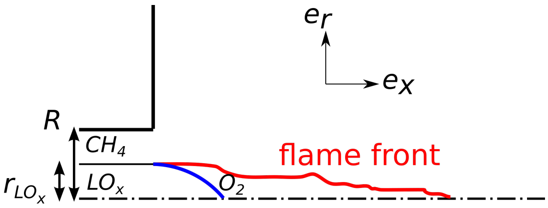

(c) Injectors geometry

Figure 1: (a) and (b) Instantaneous slice of LES results. (c) Geometry of the simplified injector. Black solid lines represent the walls. The black dotted line is the axis of symmetry of the injector. The blue curve illustrates the evaporation front of LO_x and the red one the flame front.

(H1): The injection is coaxial: an internal injection of liquid oxygen (LO_x) and an external injection of methane (CH_4). We will assume an axi-symmetric behavior of the flame.

(H2): The reactive jet flow is turbulent. We will assume that the flame will weakly modify the turbulence. As in LES, large and small scales of vortices will be considered in the present model.

(H3): In the context of high-pressure transcritical LO_x/CH_4 jet flames, assuming infinitely fast chemistry seems acceptable [1, 5, 6].

(H4): Liquid oxygen is injected and then evaporates before combustion. In the considered numerical simulations, all the oxygen is consumed. We neglect the dynamics of evaporation (driven by diffusion phenomenon [13]) and its possible interaction with combustion.

(H5): A lip is located between both injection channels (see Fig. 1a). We will neglect it, defining an equivalent radius R of the injector to conserve the same mass flow rate (see Fig. 1c).

(H6): The flow velocity, at the injection, is not strictly uniform. A model must be proposed. In the present study, we simplify it to a uniform value equal to an average of injection velocities.

(H7): To derive a model for the mixture fraction, a constant width for the mixing layer between the reactant stream is assumed. This is here valid because (1) Nez *et al.* [2, 3] observed a very small spreading rate (see also Figs. 1a and 1b) and (2) the width of the lip sets the width of the mixing layer, at least close to the injector.

3 Model for turbulent and diffusion-flame jet

3.1 Heat release rate expression integrated in the transverse plane

With the approximation of infinitely fast chemistry, the heat release rate is driven by diffusive fluxes [7]. After transverse integration, it can be expressed as a function of the mixture fraction Z [11]:

$$\dot{q}(x) = 2\pi r_{|_{Z=Z^{st}}} \Delta H_r \rho_{CH_4} D||\nabla Z|| \frac{Y_{CH_4,i}}{1 - Z^{st}} \tag{1}$$

with x the longitudinal distance from the injection inlet, ΔH_r the heat of reaction based on the equilibrium state and stoichiometric conditions (not developed here for concision), Z the mixture fraction, r the radial position, $Z^{st} = 1/(1+s)$ the mixture fraction in stoichiometric conditions ($s = Y^{st}_{LO_x}/Y^{st}_{CH_4} = 4$ the ratio of oxidant and fuel mass fraction), $Y_{CH_4,i} = 1$ the inlet mass fraction of fuel at the fuel inlet, $\rho_{CH_4} = 88$ kg/m^3 the density of the methane [2, 4] and D the diffusion coefficient defined in subsection 3.2.

For a steady jet flame within our hypotheses, the mixture fraction can be defined with the following equation [8]:

$$u\frac{\partial Z}{\partial x} = \frac{D}{r}\frac{\partial}{\partial r} r \frac{\partial Z}{\partial r} \tag{2}$$

with u the flow velocity.

3.2 Models for flow velocity and diffusivity

As a first approximation, the velocity has been expressed as an average of the injection velocities, weighted by their respective mass flow rate (deduced from quantum and mass balance equations):

$$u = \frac{\dot{m}_{LO_x,i} u_{LO_x,i} + \dot{m}_{CH_4,i} u_{CH_4,i}}{\dot{m}_{LO_x,i} + \dot{m}_{CH_4,i}} \tag{3}$$

which gives 75.67 m/s for the considered conditions [2]. To mimic the large scales of turbulence, a Gaussian distribution of velocities centered in u is considered with a standard deviation u_T given by:

$$u_T = u\sqrt{\frac{e_{lip}}{R_{inj}}} \tag{4}$$

obtained with the dimensional analysis of the momentum equation. The variables e_{lip} and R_{inj} are respectively the lip thickness (1 mm) and the radius of the injector (equal to 5 mm). The standard deviation in this configuration is approximately equal to 34 m/s, which is consistent with the turbulent kinetic energy measured by Nez *et al.* [2]. Then, to reproduce the effects of large scales on the distribution of the time-averaged heat release rate, several calculations of the heat release rate (Eq. (1)) can be performed for each velocity of the distribution, followed by an average of all the heat release rates.

The diffusion coefficient is the sum of the molecular diffusion and of the turbulent diffusion (modeling the effect of the small scales):

$$D = D_{CH_4} + D_T \tag{5}$$

with $D_{CH_4} = 2.10^{-5}$ m^2/s [9] and D_T the turbulent diffusivity discussed in following. In the community of (nonreactive) turbulent jets, it is common to model turbulent viscosity as proportional to the velocity u of the flow and the local thickness of the shear layer δ [10]. The turbulent viscosity is given by:

$$D_T = \frac{\nu_T}{Sc_T} = \frac{b}{Sc_T}\delta u \tag{6}$$

with the local shear thickness δ growing linearly with the x-position ($x = 0$ is the injector outlet):

$$\delta = \alpha x + \delta_0 \tag{7}$$

which gives:

$$D = D_{CH_4} + \frac{bu}{Sc_T}(\alpha x + \delta_0) \tag{8}$$

Nez *et al.* [2] made their numerical LES simulation with a turbulent Schmidt number Sc_T equal to 0.75. Davidson [10] proposed also a relation between α and $b = \alpha/69.2$. The spreading rate of the shear layer α can be expressed through a dimensional analysis of the continuity equation:

$$\alpha = \frac{2\rho_{CH_4}}{\rho_{CH_4} + \rho_{LO_X}}\frac{u_T}{u} \tag{9}$$

with ρ_{CH_4} the injected methane density, ρ_{LO_x} the injected LO_x density, u the mean velocity given by Eq. (3) and u_T its standard deviation expressed by Eq. (4). For this configuration, the spreading rate model gives 0.065, which is close to 0.05 measured in the simulation of Bouton *et al.* [4].

It leads to the following equation to resolve for the mixture fraction:

$$u\frac{\partial Z}{\partial x} = \frac{D_{CH_4} + \frac{bu}{Sc_T}(\alpha x + \delta_0)}{r}\frac{\partial}{\partial r}r\frac{\partial Z}{\partial r} \tag{10}$$

3.3 Analytical solution of the mixture fraction

Burke and Schumann derived a solution of Eq. (10) for a laminar diffusion jet flame ($D_T = 0$) [8]. For $Z = 1$ at the fuel inlet and $Z = 0$ at the LO_x inlet and considering the turbulent diffusion but with a very low spreading rate α, the following solution can be found:

$$Z = 1 - \frac{r_{LO_x}^2}{R^2} - \Sigma_\mu \frac{2r_{LO_x}}{R^2\mu}\frac{J_1(\mu r_{LO_x})J_0(\mu r)}{J_0(\mu R)^2}\exp\left[-\frac{\mu^2 x}{u}\left(D_{CH_4} + \frac{bu}{Sc_T}\delta_0\right)\right] \tag{11}$$

with r_{LO_x} the radius of the LO_x-channel, R the equivalent radius of the injector, without the lip (see Fig. 1c and *(H5)*), J_0 and J_1 the Bessel functions and μ the roots of $J_1(\mu R) = 0$.

4 Mixture fraction and heat release rate results

The mixture fraction formula (Eq. (11)) is implemented in a Python script to calculate the positions of the flame front ($Z = Z^{st}$), the mixture gradient and the heat release rate (Eq. (1)). In the following, we impose a local shear thickness, at $x = 0$, δ_0 equal to 0 (classical assumption, without a lip; see [10]). This implies that the spreading-rate term effect is not so small in comparison with the molecular diffusion effect. It has been neglected to derive an analytical expression for Z, but it is kept in the expression of the heat release rate (Eq. (1)).

The mixture fraction (Eq. (11)) is now plotted for the conditions of Nez *et al.* [2] (see Fig. 2a), with u given by Eq. (3). The heat release rate (Eq. (1)) is also illustrated (Fig. 2b) for the velocity given by Eq. (3) and for a gaussian distribution (see Eq. (4), with 200 values of velocity considered) and compared with the numerical simulation results of Bouton *et al.* [4] 2D coaxial LES) and Nez *et al.* [2] (a 3D LES). The discrepancies between the two simulations can be related to the spatial dimensions, to the solver used, and to physical models.

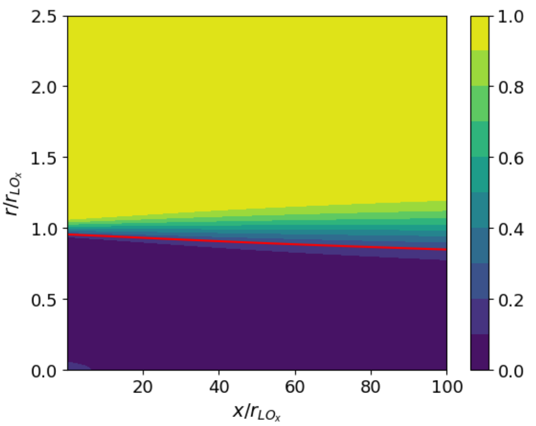

(a) Mixture fraction Z and isoline $Z = Z^{st}$ in red (flame location), for u modeled by Eq. (3)

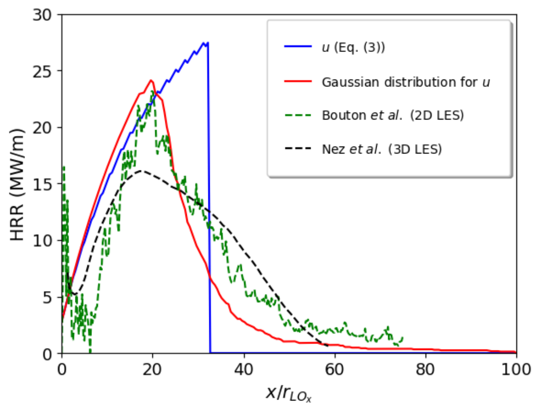

(b) Heat release rate, integrated in the transverse plane, along the x-axis

Figure 2: Model results. The models of heat release rate are compared to the numerical LES databases [2,4]

The mixture fraction, in the r-x coordinates system, illustrates the flame position by the red curve ($Z = Z^{st}$) showing an under-ventilated flame, as expected (LO_x is completely consumed in the LES simulations). The heat release rate is evaluated with the diffusive flux through this red curve (representing a surface, Eq. (1)), with two expressions of flow velocity (see Fig. 2b). The one with the label u (blue curve) corresponds to Eq. (3). The second (red curve) is an average of heat release rates for which the velocity is randomly evaluated with a Gaussian distribution (see subsection 3.2). The step, far from the injector, for the first model (blue curve) is a direct consequence of the total consumption of the injected oxygen. It gives a flame length close to $30/r_{LO_x}$. The second model (red curve) is smoother, far from the injector, because each velocity of the Gaussian distribution leads to a different flame length.

The global heat release rates (integration over x) of the numerical databases (green and black curves) and the present models (red and blue ones) are equal, validating the sub-model of chemistry equilibrium (computation of ΔH_r). Very close to the injector ($x/r_{LO_x} < 10$), the models do not fit very well to the simulation results, but the flow in this zone is quite complex due to the lip. Downstream, for $10 < x/r_{LO_x} < 20$, the derivatives of the models are correct in comparison to the simulations. Finally, the end of the flame ($20 < x/r_{LO_x} < 80$) is much better represented by the model considering a Gaussian distribution for the flow velocity.

5 Conclusion

In the state of the art of liquid rocket injector, the heat release rate is modeled by a rectangular function with three degree of freedom [2]. Despite numerous but relevant assumptions, everything is modeled with a rather convincing distribution for the heat release rate, compared to LES numerical simulations. This model of longitudinal distribution of the heat release rate, based on infinitely fast chemistry, includes several sub-modelings: (a) a turbulent diffusion model, (b) a model for the mean velocity, (c) a model for large turbulent scale, (d) a model for the heat of reaction based on the equilibrium state,

(e) a model for the spreading rate, and (f) a model for the mixture fraction. The quality of the model results implies that, for this operating point, the combustion process is controlled by the turbulent and molecular Peclet numbers and the turbulent intensity. In future work, the mixture fraction will be resolved numerically and compared to the analytical expression, and then the model of the heat release rate will be validated with other LES simulations of diffusion flames in transcritical turbulent jets, for liquid rocket injectors, and, finally, used to complement analytical models of flame transfer functions derived in the state-of-the-art.

Acknowledgments

This work is dedicated to the memory of Laurent Jacquin (1959-2024). AG and MB thank Aurélie Nicole, Guillaume Ribert, and Marie Théron for fruitful discussions about LO_x/CH_4 flames in the framework of MB's PhD thesis.

References

[1] Candel S, Schmitt T, Darabiha N. (2011). Progress in transcritical combustion: experimentation, modeling and simulation. In *23rd ICDERS*, 111.

[2] Nez R, Schmitt T, Gonzalez-Flesca M, Candel S, Ducruix S. (2017). Response of a transcritical coaxial flame to fuel injection rate modulations: Analysis and low-order modeling of the generation of unsteady heat release rate. In *7th European Conference for Aeronautics and Aerospace Sciences*.

[3] Nez R, Schmitt T, Ducruix S. (2018). High-frequency combustion instabilities in liquid rocket engines driven by propellants flow rate oscillations. In *3AF SpacePropulsion 2018 Conference*.

[4] Bouton M, Genot A, Nicole A, Ribert G. (2024). Flame dynamics under methane injection modulations in a transcritical coaxial flow. In *3AF SpacePropulsion 2024 Conference*.

[5] Pons L, Darabiha N, Candel S. (2008). Pressure effects on non-premixed strained flames. Combust. Flame, 152: 218.

[6] Pons L, Darabiha N, Candel S, Ribert G, Yang V. (2009). Mass transfer and combustion in transcritical non-premixed counterflows. Combust. Theor. Model., 13: 57

[7] Poinsot T, Veynante D. (2005). Theoretical and numerical combustion, RT Edwards, 2005

[8] Burke S, Schumann T. (1928). Diffusion flames. Ind. Eng. Chem., 20: 998

[9] Massman W. (1998). A review of the molecular diffusivities of H2O, CO2, CH4, CO, O3, SO2, NH3, N2O, NO, and NO2 in air, O2 and N2 near STP. Atmos. Environ., 32: 1111

[10] Davidson P. (2015). Turbulence: an introduction for scientists and engineers. Oxford university press.

[11] Williams F A. (1985). Combustion theory. Benjamin Cummings, Menllo Park, CA.

[12] Zong N, Yang V. (2006). Cryogenic fluid jets and mixing layers in transcritical and supercritical environments. Combust Sci. Technol., 178: 193.

[13] Yang V. (2000). Modeling of supercritical vaporization, mixing, and combustion processes in liquid-fueled propulsion systems. Proc. Combust. Inst., 28: 925.